

A new bridge-vehicle system part I : Formulation and validation

Tommy H.T. Chan†

*Department of Civil and Structural Engineering, The Hong Kong Polytechnic University,
Hungghom, Kowloon, Hong Kong*

Ling Yu‡

*Blasting and Vibration Research Department, Yangtze River Scientific Research Institute,
23 Huangpu Street, Wuhan, Hubei, 430010, P.R. China*

T.H. Yung‡‡

T.Y. Lin, Hong Kong, Consulting Engineers Ltd., Hong Kong

Jeffrey H.F. Chan‡‡

Wong and Ouyang (Civil & Structural Engineering) Ltd., Hong Kong

(Received May 22, 2000, Revised March 22, 2002, Accepted December 6, 2002)

Abstract. This paper presents the formulation of a new bridge-vehicle system with validation using the field data. Both pitching and twisting modes of the vehicle are considered in the contribution of the dynamic effects in the bridge responses. A heavy vehicle was hired as a control vehicle with known axle weight, axle spacing and spring coefficients. The measured responses were generated from the control vehicle running at a particular speed at a test span at Ma Tau Wai Flyover. The measured responses were acquired using strain gauges installed beneath the girder beams of the test bridge. The simulated responses were generated using BRVEAN that is a self-developed program based on the proposed bridge-vehicle system. The validation shows that the bridge model is valid for representing the test bridge and the governing equations are valid for representing the motion of moving vehicles.

Key words: bridge-vehicle interaction; dynamic responses; eccentric beam model; Fast Fourier Transform; field test; impact on bridges; surface roughness; tire-suspension system.

† Associate Professor

‡ Senior Engineer

‡‡ Assistant Structural Engineer

‡‡ Civil Engineer

1. Introduction

The responses induced by static loads are called static responses. Previous researchers observed that responses, e.g., bending moments, induced from vehicles running across beams are larger than the static responses due to dynamic effects. Willis (1849) suggested the first analytical approach to the railway bridge vibration problem. He derived a differential equation to calculate the deflection of a massless beam subjected to a moving load with a constant velocity. Stokes (1896) and Zimmermann (1896) solved the differential equation using different approaches. Numerous analytical studies (Krylov 1905, Timoshenko 1911, Jeffcott 1929, Inglis 1934, Stauding 1934, Lowan 1935, Schallenkamp 1937, Looney 1944, Odman 1948, Ayre *et al.* 1950, Wen 1960, Fleming and Romauldi 1961) were then carried out to formulate equations to predict the dynamic responses on beams. Fryba (1968) extensively studied vibration analysis of a simply supported beam subjected to various kinds of moving loads. After computers came into wide use in the mid-1950's, studies on bridge dynamics became more complete and realistic. Numerous studies investigating bridge-vehicle interaction by means of the finite element method (Hayashikawa and Watanabe 1981, Hino *et al.* 1984, Olsson 1985, Inbanathan and Wieland 1987, Wu *et al.* 1987, Taheri and Ting 1990, Lin and Trethewey 1990, Fafard *et al.* 1993, Mabsout *et al.* 1997, Yang and Yau 1997, Kou and DeWolf 1997), the finite strip method (Smith 1973, Hutton and Cheung 1979, Mulcahy 1983), and other methods (Lagrange multipliers [Blejwas *et al.* 1979], grillage analysis [Jaeger and Bakht 1982], infinite continuous beam [Cai *et al.* 1988], structural impedance method [Taheri and Ting 1989], Lagrange-Ritz method [Klasztorny and Langer 1990], and improved matrix method [Metwally *et al.* 1993]) were published. However, these studies considered only one vibration mode of vehicles to the dynamic responses on simple one- or two-dimensional bridge models. Even though three-dimensional models were used recently (Chatterjee *et al.* 1994, Tan *et al.* 1998 and Fafard *et al.* 1998) their efficiency and accuracy has the potential to increase. As the mechanisms between a bridge and a vehicle is very complicated, there is a need to develop a model to predict the dynamic responses on bridges.

This paper presents a study on the formulation of a bridge-vehicle system and the validation of the system using the field data measured from an existing prestressed concrete bridge. The validation is to compare between the measured and simulated responses. The simulated responses were obtained using BRVEAN, which is a computer program written using FORTRAN. The BRVEAN is an acronym derived from BRidge-VEhicle system ANalysis and was implemented basing on the finite element formulation of quadrilateral flat shell elements with eccentric beam stiffeners.

2. Governing equations

2.1 Vehicle modelling

The bridge-vehicle system of the present study models the vehicle as a two-axle (front and rear axles), four-wheel (each axle consists of two wheels) system as shown in Fig. 1. The body of the vehicle is represented as a rigid body of mass M_v . The frame, axles and wheels are approximated by concentrated point masses attached to the top of the suspension system. For each tire-suspension system, the bottom spring represents the tire elasticity (k_t) and the top spring denotes the suspension

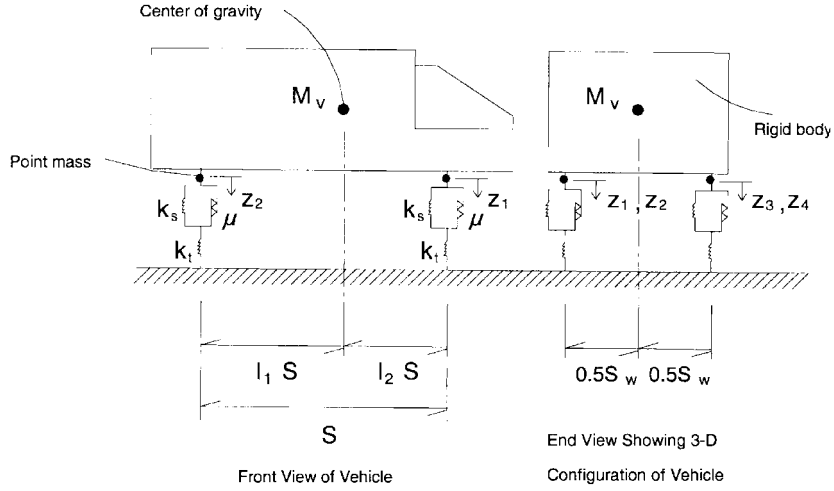


Fig. 1 Idealized 3-D vehicle model

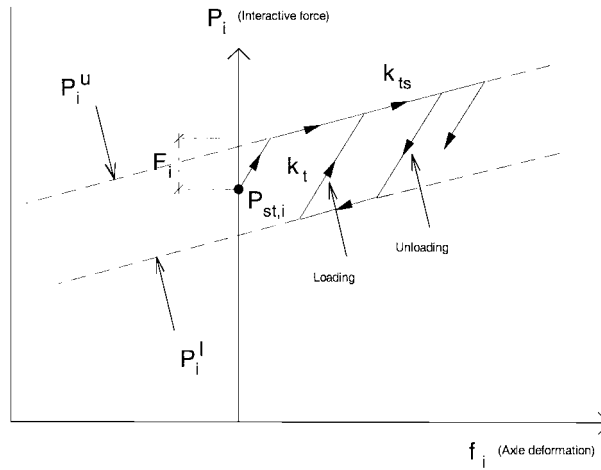


Fig. 2 Load-deformation relationship for i^{th} axle of the vehicle

elasticity (k_s). In addition, a frictional device is attached in parallel with the suspension spring to simulate the interleaf friction (μ) in the leaf-type suspension spring.

2.2 Tire-suspension system

Because of the effect of interleaf friction in the suspension spring, the load-deformation ($P_i - f_i$) relationship for the springs is represented by a bilinear diagram of the hysteretic type by Veletsos and Huang (1970) and is shown in Fig. 2. P_i is the interacting force of the i^{th} axle, and f_i is the deformation of the i^{th} axle given by:

$$f_i = z_i - r_i - b_i \tag{1}$$

where z_i is the vertical displacement of the i^{th} axle as shown in Fig. 1 (+ve downwards), r_i is the road surface roughness under the i^{th} axle (+ve downwards) and b_i is the bridge vertical displacement under the i^{th} axle (+ve downwards).

As mentioned earlier, the bridge is modeled by shell with eccentric beam elements (Chan and Chan 1994). In most situations, the position of the i^{th} axle is within the shell element of the bridge. Therefore, b_i can be evaluated as:

$$b_i = [N^s]_i^T [w^s]_i \quad (2)$$

where $[N^s]_i$ is the matrix of element shape function of the shell element evaluated at the position of the i^{th} axle and $[w^s]_i$ is the vertical nodal displacement of the corresponding shell element.

Only the tire spring is activated when the interactive force is less than the limiting friction force F_i . The limiting friction force is given by:

$$F_i = \mu P_{st,i} \quad (3)$$

where μ is a dimensionless coefficient, referred to as the ‘‘coefficient of interleaf friction’’ and $P_{st,i}$ is the force exerted by the i^{th} axle load when the vehicle is in its position of static equilibrium. At any instant, if the suspension spring engages, the effective stiffness of the tire-suspension system becomes equal to the stiffness, k_{ts} , such that the reciprocal of k_{ts} is equal to the sum of the reciprocals of k_s - the suspension spring and k_t - the tire spring stiffness.

Referring to the force-deformation ($P_i - f_i$) diagram shown in Fig. 2, the upper and lower portions of the skeleton curve can be represented by Eqs. (4) and (5) respectively:

For line P_i'' (upper portion of the skeleton curve):

$$P_i = k_{ts} f_i + P_{st,i} \left(1 + \mu \left(1 - \frac{k_{ts}}{k_t} \right) \right) \quad (4)$$

For line P_i' (lower portion of the skeleton curve):

$$P_i = k_{ts} f_i + P_{st,i} \left(1 - \mu \left(1 - \frac{k_{ts}}{k_t} \right) \right) \quad (5)$$

It can be noted that the two lines are parallel with slope k_{ts} .

2.3 Pitching and twisting motion of the vehicle

The vehicle model considered in this study is a 3-D model that is different from the 2-D planer model by Veletsos and Huang (1970). For a 3-D model, the forces in the axles/wheels at any time depend upon both the pitching and twisting motion of the vehicle.

The pitching motion of vehicle is considered by Chatterjee *et al.* (1994). The changes of the interacting force at node 1 can be obtained by applying separately

$$\ddot{z}_1 = \ddot{z}_3 = 1 \quad \text{and} \quad \ddot{z}_2 = \ddot{z}_4 = 1 \quad (6)$$

and considering the total force acting on the node:

$$(P_{st,1} - P_1) = l_1 \frac{M_v}{2} (l_1 \ddot{z}_1 + l_2 \ddot{z}_2) + \frac{m_l}{2} (\ddot{z}_1) + \frac{M_v R_P^2}{2 S^2} (\ddot{z}_1 - \ddot{z}_2) \quad (7)$$

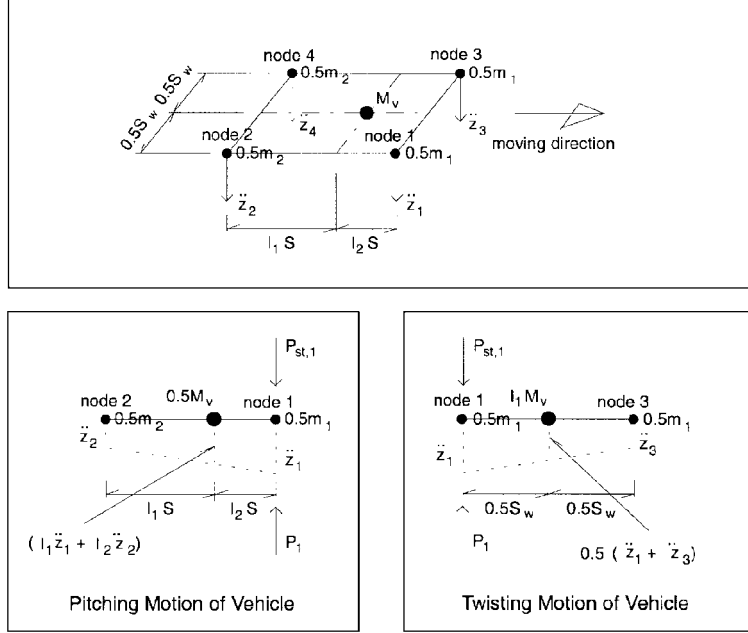


Fig. 3 Idealized 3-D vehicle

where S is the axle spacing of the vehicle, M_v is the mass of the vehicle body, m_1 is the total mass of the front axle, R_p is the radius of gyration of the vehicle body about an axis which passes through the center of gravity for pitching motion, and l_1, l_2 are the dimensionless parameters defining the position of center of gravity for pitching motion as shown in Fig. 3. Similar equations can be obtained for nodes 2 to 4 in Fig. 3 and let M_{vt} be the total mass of the vehicle including the total mass of two axles, namely, $M_{vt} = M_v + m_1 + m_2$, here, m_2 is the total mass of the rear axle. The four equations can be combined and expressed as:

$$-M_{vt} \begin{bmatrix} v_{11}^p & v_{12}^p & v_{11}^p & v_{12}^p \\ v_{21}^p & v_{22}^p & v_{21}^p & v_{22}^p \\ v_{11}^p & v_{12}^p & v_{11}^p & v_{12}^p \\ v_{21}^p & v_{22}^p & v_{21}^p & v_{22}^p \end{bmatrix} \begin{Bmatrix} \ddot{z}_1 \\ \ddot{z}_2 \\ \ddot{z}_3 \\ \ddot{z}_4 \end{Bmatrix} = \{P\} - \{P_{st}\} \quad (8)$$

or

$$-M_{vt} [V^p] \{\ddot{Z}\} = \{P\} - \{P_{st}\} \quad (8a)$$

in which $\{\ddot{Z}\} = \{\ddot{z}_1 \ \ddot{z}_2 \ \ddot{z}_3 \ \ddot{z}_4\}^T$ is the vector of vertical displacements (here, superscript T indicates transpose of matrix), $[V^p]$ is the coefficient matrix consists of $v_{ij}^p (i, j = 1, 2)$, $\{P\} = \{P_1 \ P_2 \ P_3 \ P_4\}^T$ is the vector of interacting forces, $\{P_{st}\} = \{P_{st,1} \ P_{st,2} \ P_{st,3} \ P_{st,4}\}^T$ is the vector of static axle-load and

$$v_{ii}^p = \left(l_i^2 + \frac{R_p^2}{S^2} \right) \frac{M_v}{2M_{vt}} + \frac{m_i}{2M_{vt}} \quad (9)$$

and

$$v_{12}^p = v_{21}^p = \left(l_1 l_2 - \frac{R_p^2}{S^2} \right) \frac{M_v}{2M_{vt}} \quad (10)$$

where $i = 1$ or 2 .

Similarly, in the consideration of the twisting motion of the vehicle, the whole vehicle is assumed as a rigid body and rotating about its longitudinal axis. Applying the changes of interactive force at node 1 and referring to Fig. 3, the equation of motion for motion for rotational equilibrium is:

$$\begin{aligned} S_w(P_{st,1} - P_1) &= S_w \frac{m_1 \ddot{z}_1 + m_2 \ddot{z}_2}{2} + \frac{S_w}{2} M_v \left(\frac{\ddot{z}_1 + \ddot{z}_3}{2} l_1 + \frac{\ddot{z}_2 + \ddot{z}_4}{2} l_2 \right) \\ &+ M_v R_t^2 \left(\frac{\ddot{z}_1 - \ddot{z}_3}{S_w} l_1 + \frac{\ddot{z}_2 - \ddot{z}_4}{S_w} l_2 \right) \end{aligned} \quad (11)$$

where S_w is the axle spacing of the vehicle in transverse direction and R_t is the radius of gyration of the vehicle about a longitudinal axis that passes through the center of gravity. Applying the same procedures for nodes 2 to 4 and combining the four equations, the equations of twisting motion of the vehicle can be expressed as:

$$-M_{vt} \begin{bmatrix} v_{11}^t & v_{12}^t & v_{13}^t & v_{14}^t \\ v_{11}^t & v_{12}^t & v_{13}^t & v_{14}^t \\ v_{13}^t & v_{14}^t & v_{11}^t & v_{12}^t \\ v_{13}^t & v_{14}^t & v_{11}^t & v_{12}^t \end{bmatrix} \begin{Bmatrix} \ddot{z}_1 \\ \ddot{z}_2 \\ \ddot{z}_3 \\ \ddot{z}_4 \end{Bmatrix} = \{P\} - \{P_{st}\} \quad (12)$$

or

$$-M_{vt} [V^t] \{\ddot{Z}\} = \{P\} - \{P_{st}\} \quad (12a)$$

where, $[V^t]$ is the coefficient matrix consists of $v_{1j}^t (j = 1, 2, 3, 4)$, and

$$v_{1j}^t = \left(\frac{1}{4} + \frac{R_t^2}{S_w^2} \right) l_j \frac{M_v}{M_{vt}} + \frac{m_i}{2M_{vt}}; (j = 1, 2) \quad (13)$$

and

$$v_{1j}^t = \left(\frac{1}{4} - \frac{R_t^2}{S_w^2} \right) l_{j-2} \frac{M_v}{M_{vt}}; (j = 3, 4) \quad (14)$$

By combining the equations of the pitching motion and the twisting motion of the vehicle, and let $[V] = [V^p] + [V^t]$, the equations of motion of the vehicle can be written as:

$$-M_{vt} [V] \{\ddot{Z}\} = \{P\} - \{P_{st}\} \quad (15)$$

3. Bridge-vehicle interaction model

When the interactive force P_i between the road surface (shell element) and the i^{th} wheel is converted to equivalent nodal forces using the principle of virtual work, the equation of motion for the bridge is written as:

$$[M]\{\ddot{d}^s\} + [C]\{\dot{d}^s\} + [K]\{d^s\} = \sum_{i=1}^4 [N^s]_i^T P_i \quad (16)$$

where $[M]$, $[C]$, $[K]$ are the global structural mass matrix, damping matrix and stiffness matrix of the bridge model respectively; d represents the nodal displacement of the bridge; $[N_s]_i$ is the element shape functions of shell element evaluated at the position of the i^{th} wheel/axle, and it is time dependent as the i^{th} wheel moves from one position to another position, and P_i is the interactive force between the bridge and the i^{th} axle.

3.1 Road surface roughness

A road surface roughness may be considered as a realization of a random process that can be described by a power spectral density (PSD) function. Typical PSD function can be described approximately by an exponential function (Hwang and Nowak 1991) as follows,

$$S(\Omega) = A_r \Omega^{-n} \quad (17)$$

where $S(\Omega)$ = PSD value for the surface roughness (m^3/cycle), A_r = roughness coefficient, n = spectral shape index and Ω = spatial frequency (cycles/m). Honda and Kajikawa (1982) measured the road surface roughness of 84 lines on 56 bridges and showed that the values of A_r could be used to relate the international roughness index (IRI), e.g., A_r of 0.64×10^{-6} cycle/m corresponded to an IRI of 6.0 for a general road surface roughness. This value of A_r was also adopted in the present study.

Regarding the road surface roughness r_i as appeared in Eq. (1), it can be generated by an inverse Fourier transforms as (Yang 1986),

$$r(t) = \sum_{n=1}^N \sqrt{4S(\Omega_n)\Delta\Omega} \cos(\Omega_n t - \theta_n) \quad (18)$$

which is the basis for generating the artificial sample functions from a given ensemble PSD function $S(\Omega_n)$ of a stationary ergodic process. Where, t = time, θ_n = a random phase angle uniformly distributed from 0 to 2π , Ω_n = a circular frequency within the interval in which the PSD function is defined. $\Delta\Omega$ = frequency increment that is defined as $\Delta\Omega = (\Omega_{\max} - \Omega_{\min})/N$, here N = the total number of frequency increment in the range $(\Omega_{\min}, \Omega_{\max})$, and Ω_{\min} and Ω_{\max} = the lower and upper bounds between which the PSD function is defined. The frequency Ω_n is computed by interpolation as $\Omega_n = \Omega_{\min} + \Delta\Omega(n-1)$. In general, the road surface roughness computed from Eq. (18) is different depending on the random numbers θ_n used. The random roughness field is assumed to be fully correlated over the width of the deck (Chatterjee *et al.* 1994).

3.2 Solution method

Applying the Newmark Method to Eq. (16), the effective stiffness matrix and the effective loads at time $t + \Delta t$ for the equation of motion of the bridge can be written as:

$$(a_0[M] + a_1[C] + [K])\{d^s\}_{t+\Delta t} = [M](a_0\{d^s\}_t + a_2\{\dot{d}^s\}_t + a_3\{\ddot{d}^s\}_t) + [C](a_1\{d^s\}_t + a_4\{\dot{d}^s\}_t + a_5\{\ddot{d}^s\}_t) + \sum_{i=1}^4 [N^s]_i^T P_{i,t+\Delta t} \quad (19)$$

where a_i are the integration constants of Newmark method.

Similarly, the equation of the effective stiffness matrix and the loads vector for the vehicle is

$$-a_0 M_{vt} [V] \{z\}_{t+\Delta t} = -M_{vt} [V] (a_0 \{z\}_t + a_2 \{\dot{z}\}_t + a_3 \{\ddot{z}\}_t) + \{P\}_{t+\Delta t} - \{P_{st}\} \quad (20)$$

The unknown variables at time are $t + \Delta t$, $[d^s]_{t+\Delta t}$, $[z]_{t+\Delta t}$ and $[P]_{t+\Delta t}$. However, because of the bilinear nature of the force-deformation relationship of the suspension system of the vehicle, the interactive forces are not available as explicit function of time, and an iterative procedure is required. The steps are presented below.

1. At any time $t + \Delta t$, define the longitudinal position of each axle of the vehicle. Obtain the values of z_i , d_i^s and their derivatives of the vehicle and bridge, interacting forces P_i at the previous time instant t .
2. Solve the vehicle equations of motion. Obtain z_i and their derivatives at time instant $t + \Delta t$ by Eqs. (21) and (22):

$$\{\ddot{z}\}_{t+\Delta t} = a_0(\{z\}_{t+\Delta t} - \{z\}_t) - a_2\{\dot{z}\}_t - a_3\{\ddot{z}\}_t \quad (21)$$

$$\{\dot{z}\}_{t+\Delta t} = \{\dot{z}\}_t + a_6\{\ddot{z}\}_t + a_7\{\ddot{z}\}_{t+\Delta t} \quad (22)$$

3. Solve the bridge equations of motion. Obtain d_i^s and their derivatives at time instant $t + \Delta t$ by Eqs. (23) and (24):

$$\{\ddot{d}\}_{t+\Delta t} = a_0(\{d\}_{t+\Delta t} - \{d\}_t) - a_2\{\dot{d}\}_t - a_3\{\ddot{d}\}_t \quad (23)$$

$$\{\dot{d}\}_{t+\Delta t} = \{\dot{d}\}_t + a_6\{\ddot{d}\}_t + a_7\{\ddot{d}\}_{t+\Delta t} \quad (24)$$

4. Find the values of b_i by Eq. (2).
5. Determine $f_{i,t+\Delta t}$, the deformation of the i^{th} axle at $t + \Delta t$ by Eq. (1) using the latest available values of z_i and b_i . The value of r_i is computed from the synthetically generated bridge pavement profile.
6. Compute a new set of P_i at time instant $t + \Delta t$ as:

$$P_{i,t+\Delta t} = P_{i,t} + \Delta P_i \quad (25)$$

where $P_{i,t+\Delta t}$ is the value of P_i at $t + \Delta t$, $P_{i,t}$ is the value of P_i at t , and ΔP_i is the change in P_i in the interval between t and $t + \Delta t$. Making reference to Veletsos and Huang's work (1993), ΔP_i can be evaluated as follows:

- a. Consider a point on the $P_i - f_i$ diagram representing the condition of the axle at time t . This point is represented by values of $P_{i,t}$ and $f_{i,t}$ at time t (Fig. 2).
- b. Consider a straight line with slope k_t and passing through this point, and let $f_{i,t}^u$ and $f_{i,t}^l$ represent the abscissas of the points of intersection of this line with upper and lower portions of the skeleton curve respectively.
- c. Making use of Eqs. (4) and (5), the values of $f_{i,t}^u$ and $f_{i,t}^l$ can be found by Eqs. (26) and (27).

$$f_{i,t}^u = \frac{k_t f_{i,t} - P_{i,t} + P_{st,i} \left(1 + \mu \left(1 - \frac{k_{ts}}{k_t} \right) \right)}{k_t - k_{ts}} \quad (26)$$

$$f_{i,t}^l = \frac{k_t f_{i,t} - P_{i,t} + P_{st,i} \left(1 - \mu \left(1 - \frac{k_{ts}}{k_t} \right) \right)}{k_t - k_{ts}} \quad (27)$$

- d. After obtaining the values of $f_{i,t}^u$ and $f_{i,t}^l$, and with the value of $f_{i,t+\Delta t}$ available in step 5, the change in the interacting force, ΔP_i , is determined from the following relations:

$$\text{if } f_{i,t}^l \leq f_{i,t+\Delta t} \leq f_{i,t}^u, \quad \Delta P_i = k_t (f_{i,t+\Delta t} - f_{i,t}) \quad (28)$$

$$\text{if } f_{i,t+\Delta t} > f_{i,t}^u, \quad \Delta P_i = k_t (f_{i,t}^u - f_{i,t}) + k_{ts} (f_{i,t+\Delta t} - f_{i,t}^u) \quad (29)$$

$$\text{if } f_{i,t+\Delta t} < f_{i,t}^l, \quad \Delta P_i = k_t (f_{i,t}^l - f_{i,t}) + k_{ts} (f_{i,t+\Delta t} - f_{i,t}^l) \quad (30)$$

7. Compare the values of P_i from step 6 with that of using steps 2 and 3. If the difference between the two steps of values of interaction force P_i is greater than a prescribed tolerance (0.001 in this study), repeat steps 2 through 7 till the values of P_i converge. Always use latest available values of P_i , z_i , d_i^s and f_i .
8. Once the convergence is achieved for any time instant, obtain the bridge displacements and calculate the bending moment at any required section. Up to this, the iteration for the time interval under consideration is completed. Proceed to next time interval and repeats the process.

The above bridge-vehicle interaction model is implemented into a computer program called BRVEAN.

4. Verification program

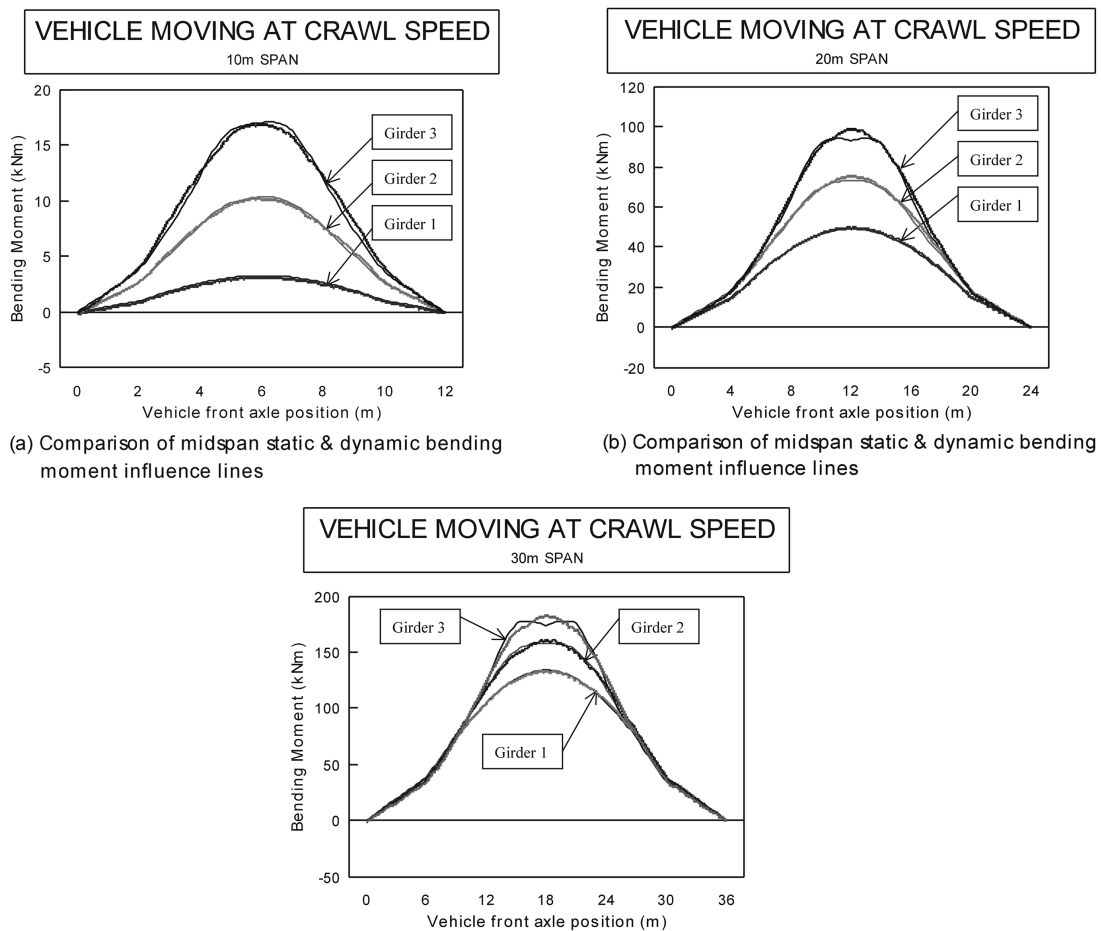
In order to validate the proposed bridge-vehicle system, three validations have been conducted separately, one based on theoretical studied and the other two based on experimental validations.

4.1 Theoretical validation

In the theoretical validation, three virtual bridge models with different span lengths are employed. All bridges have an overall width of 11.25 m and consist of five equally spaced identical girders that are simply supported. One case is to be studied at each bridge model. In each case, a single vehicle moves across the bridge on the central girder with a crawl speed of 2 m/s. A summary of

Table 1 A summary of parameters of three bridge models

Span (m)	Mass per unit length of bridge (kg/m)	Flexural rigidity of bridge (10^9 Nm^2)	Fundamental frequency of bridge (Hz)	Mass of vehicle (kg)	Axle distance of vehicle (m)	Tire stiffness of vehicle (N/m)
10	4526.25	1.89	10.15	2263	2	556240
20	8613.5	14.45	5.09	8614	4	531324
30	8613.5	31.66	3.35	12920	6	353498



(c) Comparison of midspan static & dynamic bending moment influence lines

Fig. 4 Comparison of typical static and dynamic influence lines

parameters of the three bridges is shown in Table 1.

The static influence lines of the bridge subject to moving loads are calculated using another self-developed and validated program STCAR (Chan 1996). Both displacement and bending moment influence lines are calculated at the section of mid-span for each girder unit. The dynamic influence

Table 2 A summary of the simulated and measured responses

Vehicle speed (m/s)	Simulated response (kN.m)	Measured response (kN.m)
6	296	305
12	299	310
18	311	315
24	302	320
30	331	330

lines of the bridge subject to a vehicle moving at a crawl speed are calculated by BRVEAN and are compared to the results generated by the program STCAR. A comparison between the static and dynamic influence lines is illustrated in Fig. 4 for different span of bridges. The results show that the static influence lines and the dynamic influence lines for crawl speed are nearly identical therefore BRVEAN is valid.

4.2 Six mile creek bridge

The Six Mile Creek Bridge with a span length of 11.28 m is simply supported composite steel and concrete bridge. The 180 mm thick concrete slab is supported on six rolled steel joists 610 mm × 190 mm × 140 kg/m (Chan and O'Connor 1990, O'Connor and Pritchard 1985, Swannell and Miller 1987). The test vehicle (Swannell and Miller 1987) is a two-axle International ACCO 1950A truck with a 3.124 m wheel base. For the case of fully loaded, the rear axle load is 9150 kg and the front axle load is 4650 kg. The values of suspension stiffness and tire stiffness are 250 kN/m and 1564 kN/m respectively.

A comparison of the mid-span bending moments between measured results from the Six Mile Creek bridge and simulated responses from BRVEAN are tabulated in Table 2. Table 2 shows that acceptable responses with the measured responses can be simulated using BRVEAN.

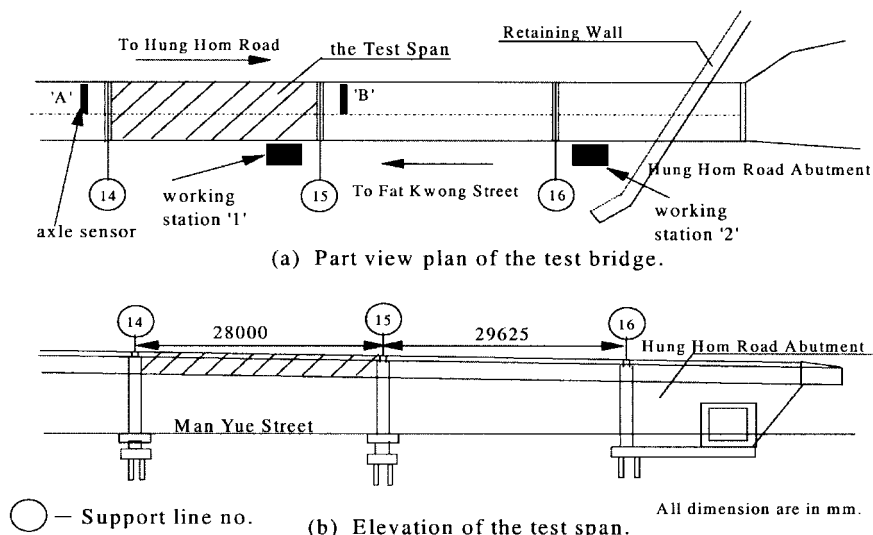


Fig. 5 A plan and elevation of the test bridge

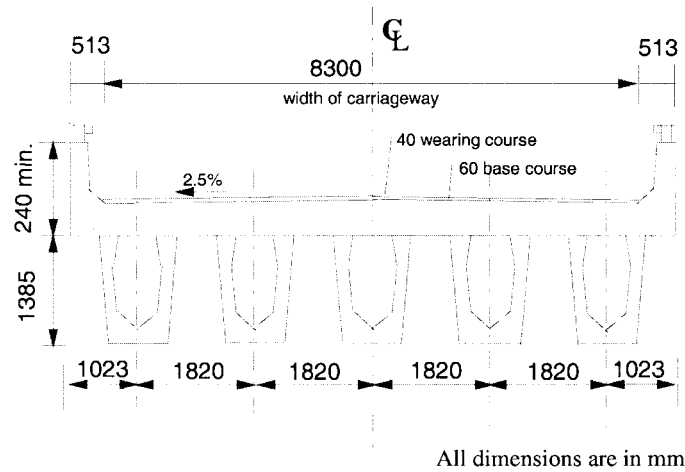


Fig. 6 A cross-sectional view of the test span

4.3 Ma Tau Wai Flyover

4.3.1 Test bridge

After a prolonged study on considering practicality of instrumentation, traffic flow and a span to width ratio, an existing prestressed concrete highway bridge was selected for the present study. The test bridge was Ma Tau Wai Flyover linking Fat Kwong Street and Hung Hum Road in Kowloon, Hong Kong (Fig. 5). The test bridge is a dual carriageway slab-on-girder bridge. Each girder has four tendons in two groups. Group one is the two outside tendons with a prestressing force of 2320 kN and group two is the two inner tendons with a prestressing force of 2430 kN. A typical section of the test bridge is shown in Fig. 6. The second span away from the Hung Hum Road abutment was selected to be a test span. It has a span length of 28 meters and 9.326 meters wide.

4.3.2 Control vehicle

A 2-axle heavy vehicle was hired to be a control vehicle. The control vehicle was manufactured from Nissan in 1984 with a model number of CKB21N-00098. It was loaded with a total weight of 15380 kg. The front and rear axle weights were 6520 kg and 8860 kg. The suspension system of the control vehicle has the spring coefficients of 22 kg/mm and 26 kg/mm (main) for the front axle and 81 kg/mm (total) for the rear axle. The central line of control vehicle coincided with the central line of carriageway when it crossed the test bridge.

4.3.3 Data acquisition system

A set of data acquisition system was used in the field measurement. It consisted of four elements, i.e., a sensing element, a conditioning element, a converting element, and a display element. All instruments were located in a control room.

4.3.3.1 Sensing element

Strain gauges and axle sensors were used to be the sensing elements. The strain gauges were to acquire the total dynamic responses of the test span as input data for a force identification study. The axle sensors were to provide an indication on entry and exit time of vehicles.

Table 3 Adjusted locations of the strain gauges measured from line no. 14

Strain gauge transverse location no.	1	2	3	4	5	6	7
Location from support line no. 14 (mm)	3215	6765	10315	13866	17416	21210	24516

Thirty-five strain gauges were installed beneath the bridge girders of the test span. The thirty-five strain gauges were installed along the five girders with seven strain gauges on each girder. Seven measurement channels were formed. Each measurement channel was formed by connecting five strain gauges (one strain gauge @ 120 Ω from each girder) in a series circuit. The strain gauges were initially planned to be at equal spacing along the five girders, but this could not be achieved due to bad working conditions. The final locations of the strain gauges were checked using a surveying technique after the installation. The adjusted locations of the strain gauges are tabulated in Table 3.

Four axle sensors were initially installed on both traffic lanes. After a day of data-acquisition experience, it was decided to use only two of the axle sensors. Positions of the two axle sensors are shown in Fig. 5(a).

4.3.3.2 Conditioning element

A conditioning element consisted of a Wheatstone bridge circuit and an amplifier. The Wheatstone bridge circuit converts the change in the electrical resistance to the change in the voltage as output data. The Wheatstone bridge circuit was a constant current type with an active arm of 600 Ω (5 gauges @ 120 Ω). An amplifier from the Kyowa Electrical Instruments Company Limited with a model number of CDA-230A was used to amplify the measured signal after the conversion from resistance to voltage to a certain measurable level.

4.3.3.3 Converting element

One converter from the Data Translation with a model number of DT2829 was used. The converter supports measurements using either 16-channel single ended or 8-channel differential input. The latter option was adopted. When it was to measure signals from strain gauges, the first measurement channel was connected to the axle sensors and the other seven measurement channels were formed from the seven strain gauges. Similarly, the first measurement channel was connected to the axle sensors and the other seven measurement channels were formed from the seven accelerometers when it was to measure signals from accelerometers.

4.3.3.4 Display element

A software from the Data Translation (Global Lab) was used to control the converter to acquire the dynamic responses of the test span.

5. Measurement program

As the traffic is always heavy in the daytime at Man Yue Street - the street directly below the test span (Fig. 5), instrumentation was installed during the night. Instrumentation commenced on 29th September 1995 and continued for seven nights. During the first five nights, the thirty-five strain

gauges were installed. The field measurements were conducted under normal traffic conditions for five days commencing on 8th October 1995. A system calibration, a modal test and a force identification test were performed. The test procedures and results of the system calibration and the modal test have been presented in Chan *et al.* (1998).

After the calibration test, the control vehicle ran across the test span to make a few valid samples. However, only five samples were recorded because of time restrictions. The first sample was a failure because the vehicle speed significantly varied during the measurement. The fourth sample was a failure because no signals of the axle sensors were recorded. The fifth sample was also a failure because more than one vehicle ran across the test span during the measurement. Therefore, only two samples can be used, namely Test 2 and Test 3.

6. Preliminary consideration

6.1 Bridge modelling

At the present stage, BRVEAN cannot deal with the prestressing effect of the test bridge. Chan and Yung (2000) and Chan *et al.* (2000) conducted theoretical and experimental studies on the force identification using a prestressed concrete bridge respectively. They concluded that the dynamic responses on prestressed bridges are smaller than that of non-prestressed bridges induced by vehicles. The measured responses are therefore expected to be smaller than the simulated responses. The difference between the measured and simulated responses depends on the magnitude of the prestressing force and the eccentricity of tendons. Chan and Yung (2000) did not show the relationship of the difference between the responses on non-prestressed and prestressed bridges and the magnitude of the prestressing force. As the bridge model used in their study is the same as the present study, the percentage difference given in their study will be referred as an inherent percentage difference between the simulated and measured responses. Therefore the actual percentage difference will be equal to the percentage difference calculated between the measured and simulated responses minus the inherent percentage difference. The inherent percentage difference is 4.45% at the maximum responses at the mid-span. Many reports show that the road surface roughness and the vehicle suspension are the main factors affecting bridge-vehicle interaction. As the road surface roughness was not measured in the field, it is assumed the road surface roughness having an IRI of 6.0 as given in Hwang and Nowak (1990). Affecting from the road surface roughness, it is impossible to study the accuracy of both the measured and simulated responses in the time domain directly. Based on the modal superposition theory, dynamic responses on structures, e.g., bridges, are the summation of the modal amplitude and the corresponding mode shape. The natural frequency obtained from the simulated responses should be the same as the natural frequency obtained from the measured responses. In order to study the accuracy of the simulated responses to the measured responses, both the measured and simulated responses are to be converted in the frequency domain using FFT. The torsional rigidity of the test bridge is assumed to be 10% of the flexural rigidity of the test bridge.

6.2 Vehicle modelling

For the simulation, the radii of gyration along longitudinal and transverse axis of the control

vehicle are calculated using the formulae given by MacInnis *et al.* (1997). It is assumed that the longitudinal axis of the control vehicle is parallel to the center of a carriageway of the test span so that the distance between the edge of the test span and the nearest wheel is 1.648 m. As the axle weights of the control vehicle measured by a weigh-bridge were readily included the weights of wheels, it is necessary to estimate the unsprung mass of the control vehicle for further study. Different unsprung masses were suggested from past literature, e.g., an idealized 2-axle vehicle with 450 kg (front) and 890 kg (rear) (Fafard *et al.* 1993), and 800 kg (dual-tires) and 700 kg (wide-single tires) (Cole and Cebon 1996). The sprung mass of the control vehicle is therefore conservatively assumed to be 500 kg for both the front and rear axles. Typical coefficients of tire suspension are between 1500 kN/m and 5000 kN/m. It is first assumed that the coefficient of tire suspension is the mean value of the typical coefficients so that the coefficient of tire suspension is 3250 kN/m. A sensitivity study shown in Table 4 shows that the percentage differences on maximum bending moment using other coefficients of tire suspension are acceptable indicating that the mean value of the coefficient of tire suspension is acceptable for the present study.

7. Validation

A comparison is made to study the measured and simulated responses on the test bridge. A typical plot of the measured and simulated responses is shown in Fig. 7. Similar results are obtained for Test 2. Fig. 7 shows that the profile of the simulated responses is match with the profile of the measured responses. The peaks of the simulated responses are almost at the same locations of the

Table 4 A summary of percentage differences of various tire suspensions

tire suspension (kN/m)	Percentage differences		
	1500	3250	5000
bending moment (N-m)	96314.42	102340.9	108937.2
difference (%)	-5.89	0	6.45

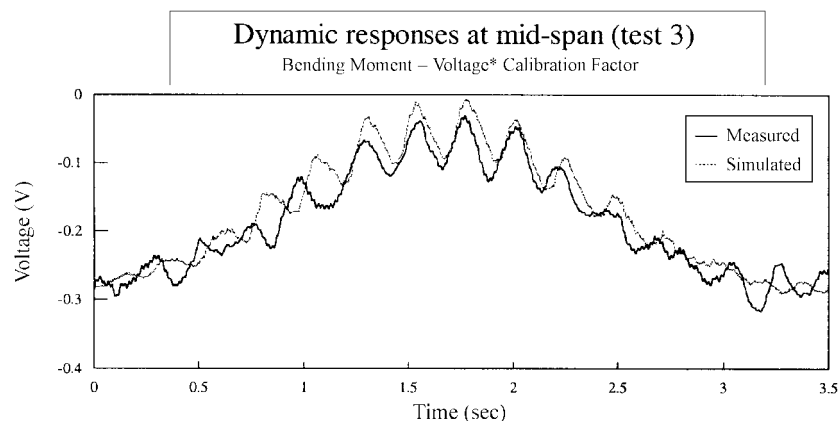


Fig. 7 A typical example of simulated and measured responses

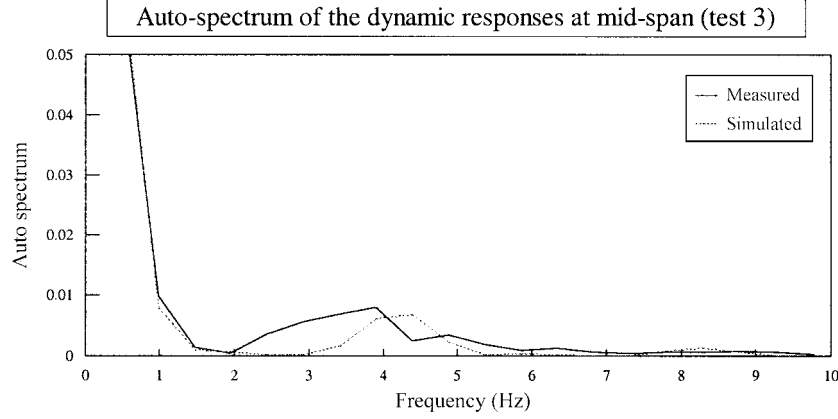


Fig. 8 A typical plot of auto-spectrum

peaks of the measured responses. As both simulated and measured responses are in the time domain, it is impossible to directly compare both simulated and measured responses at each time step to decide whether both responses agree with each other. It is known that the dynamic responses are the summation of the contribution at each vibration mode of a structure, both simulated and measured responses should have similar contribution at corresponding vibration modes. Therefore both simulated and measured responses are then converted to the frequency domain using FFT. A typical plot of auto-power spectrum is shown partly in Fig. 8.

Fig. 8 shows that there is a common peak at the frequency of 3.91 Hz. Chan *et al.* (1998) shows that the fundamental frequency of the test bridge is 4.5 Hz, which was obtained from analyzing the measured ambient vibration data. In the present study, both fundamental frequencies are obtained from analyzing the forced vibration data. The natural frequency of a beam can be estimated using the following expression.

$$\omega_i = \frac{i^2 \pi}{2L^2} \sqrt{\frac{EI}{\bar{m}}} \quad (31)$$

where ω_i is the natural frequency at the i^{th} vibration mode, L is the span length, EI is the flexural stiffness of the beam and \bar{m} is the mass per unit length. As the weight of the loaded test bridge is heavier than the un-loaded test bridge, the fundamental frequency of the test bridge of the former case will be smaller than the latter case. The result obviously shows that the accuracy of the determination of the fundamental frequency of the test bridge is affected by the vehicle. Fertis and Zobel (1961) used Rayleigh's method to determine the fundamental frequency of a structure under external loads. Rayleigh's method can be expressed as

$$\omega_t = \sqrt{\frac{g \sum_{i=1}^n W_i y_i}{\sum_{i=1}^n W_i y_i^2}} \quad (32)$$

where ω_t is the fundamental frequency of a beam, g is the coefficient of gravity, W_i is the i^{th}

external load and y_i is the deflection of the i^{th} external load. Using the expression with the consideration of the vehicle, the fundamental frequency of the test bridge is estimated as 4.32 Hz with a percentage difference of 4.0% with the measured fundamental frequency. There are two reasons causing such difference. One is the deflection of the external loads calculated without considering dynamic effects. The other is that Rayleigh's method does not take into account of the prestressing effect. However the estimation is acceptable.

It is calculated that the percentage difference between the measured and simulated responses is 10.49% at the maximum responses. The actual percentage difference is therefore 6.00% and is acceptable. On the one hand, the actual percentage difference is acceptable, on the other hand, both measured and simulated responses show having the same fundamental frequency. Therefore the proposed bridge-vehicle system is valid to predict dynamic responses on bridges.

8. Conclusions

The formulation of a new bridge-vehicle system has been given. The system has been implemented using FORTRAN, namely BRVEAN. BRVEAN has been validated using the both theoretical study and field data obtained at Six Mile Creek Bridge and Ma Tau Wai Flyover. The results of the present study show that the properties of the test bridge obtained from the test bridge (Ma Tau Wai Flyover) obtained from the modal test are valid. All three validations show that the prediction of bridge responses using the BRVEAN is feasible. By converting the bridge responses using the FFT, the fundamental frequency of the test bridge can be obtained. As BRVEAN is valid for simulating bridge responses included by a moving vehicle, it can be used for further study on bridge dynamics. A parametric study on impact on bridges has been carried out by the authors and reported in its companion paper (Chan *et al.* 2003).

Acknowledgements

This project is funded by the Hong Kong Polytechnic University Research Grants and the Research Grants Council of the Hong Kong SAR Government.

References

- Ayre, R.S., Ford, G. and Jacobsen, L.S. (1950), "Transverse vibration of a two-span beam under action of a moving constant force", *J. Appl. Mech.*, ASME, **17**, 1-12.
- Blejwas, T.E., Feng, C.C. and Ayre, R.S. (1979), "Dynamic interaction of moving vehicles and structures", *J. Sound Vib.*, **67**, 513-521.
- Cai, C.W., Cheung, Y.K. and Chan, H.C. (1988), "Dynamic response of infinite continuous beams subjected to a moving force - an exact method", *J. Sound Vib.*, **123**, 461-472.
- Chan, J.H.F. (1996), "Bridge-vehicle model for highway bridge impact studies", M.Phil Thesis, The Hong Kong Polytechnic University, Hong Kong.
- Chan, T.H.T. and Chan, J.H.F. (1994), "A finite element model on load distribution", *Development on Short and Medium Span Bridge Engineering'94*.
- Chan, T.H.T., Law, S.S. and Yung, T.H. (1998), "Modal test on an existing bridge : experience acquired",

- Transactions of HKIE*, **5**, 8-16.
- Chan, T.H.T., Law, S.S. and Yung, T.H.T. (2000), "A field study on moving force identification using an existing prestressed concrete bridge", *Engineering Structures*, **22**(10), 1261-1270.
- Chan, T.H.T. and O'Connor, C. (1990), "Wheel loads from highway bridge strains" *J. Struct. Eng. Div.*, ASCE, **16**, 1751-1771.
- Chan, T.H.T., Yu, L., Yung, T.H. and Chan, J.H.F. (2003), "A new bridge-vehicle system part II: parametric study", *Struct. Eng. and Mech., An Int. J.*, **15**(1), 21-38.
- Chan, T.H.T. and Yung, T.H. (2000), "A theoretical study of force identification using prestressed concrete bridges", *Engineering Structures*, **22**(11), 1529-1537.
- Chatterjee, P.K., Datta, T.K. and Surana, C.S. (1994), "Vibration of suspension bridges under vehicular movement", *J. Struct. Eng.*, ASCE, **120**, 681-703.
- Cole, D.J. and Cebon, D. (1996), "Truck tires, suspension design and road damage", *International Rubber Conference IRC'96*.
- Fafard, M., Bennur, M. and Savard, M. (1993), "Dynamic of bridge-vehicle interaction", *Structural Dynamics-EURODYN'93*, 951-960.
- Fafard, M., Laflamme, M., Savard, M. and Bennur M. (1998), "Dynamic analysis of existing continuous bridge", *J. Bridge Eng.*, **3**(1), 28-37.
- Fertis, D.G. and Zobel, E.C. (1961), *Transverse Vibration Theory: Application of Equivalent Systems*, the Ronald Press Company, New York.
- Fleming, J.F. and Romauldi, J.P. (1961), "Dynamic response of highway bridges", *ASCE Proceedings*, **87**(ST7), 31-61.
- Fryba, L. (1968), *Vibration of Solids and Structures Under Moving Loads*, Gronigen: Noordhoff International Publishing. (1968; revised in 1970, 1972).
- Hayashikawa, T. and Watanabe, N. (1981), "Dynamic behavior of continuous beams with moving loads", *J. Eng. Mech. Div.*, ASCE, **107**, 229-246.
- Hino, J., Yoshimura, T., Konishi, K. and Ananthanarayana, N. (1984), "A finite element method prediction of the vibration of a bridge subjected to a moving vehicle load", *J. Sound Vib.*, **96**, 45-53.
- Honda, H. and Kajikawa, Y. (1982), "Spectra of road surface roughness on bridges", *J. Struct. Eng.*, ASCE, **108**, 1956-1966.
- Hutton, S.G. and Cheung, Y.K. (1979), "Dynamic response of single span highway bridges", *Earthq. Eng. Struct. Dyn.*, **7**, 543-553.
- Hwang, E.S. and Nowak, A.S. (1991), "Simulation of dynamic load for bridges", *J. Struct. Eng.*, ASCE, **117**, 1413-1434.
- Inbanathan, M.J. and Wieland, M. (1987), "Bridge vibrations due to vehicle moving over rough surface", *J. Struct. Eng.*, ASCE, **113**, 1994-2008.
- Inglis, C.E. (1934), *A Mathematical Treatise on Vibration in Railway Bridge*, Cambridge University Press.
- Jaeger, L.G. and Bakht, B. (1982), "The grillage analogy in bridge analysis", *Canadian Journal of Civil Engineering*, **9**, 224-235.
- Jeffcott, H.H. (1929), *Phil. Mag.*, 7-8.
- Klasztorny, M. and Langer, J. (1990), "Dynamic response of single-span beam bridges to a series of moving loads", *Earthq. Eng. Struct. Dyn.*, **19**, 1107-1124.
- Krylov, A.N. (1905), "Über die erzwungen schwingungen von gleichförmigen elastischen staben", *Math Ann*, **61**.
- Kou, J.W. and DeWolf, J.T. (1997), "Vibrational behavior of continuous span highway bridge-influencing variables", *J. Struct. Eng.*, ASCE, **123**, 333-344.
- Lin, Y.H. and Trethewey, M.W. (1990), "Finite element analysis of elastic beams subjected to moving dynamic loads", *J. Sound Vib.*, **132**, 323-342.
- Looney, C.T. (1944), "Impact on railway bridges", *Bulletin series 325*, University of Illinois.
- Lowan, A.N. (1935), "On transverse oscillation of beams under the action of moving variable loads", *Philosophical Magazine*, London, **19**, Series 7, 708-715.
- Mabsout, M.E., Tarhini, K.M., Frederick, G.R. and Tayar, C. (1997), "Finite element analysis of steel girder highway bridges", *J. Bridge Eng.*, ASCE, **2**, 83-87.
- Maclnnis, D.D., Cliff, W.E. and Lsing, K.W. (1997), "A comparison of moment of inertia estimation techniques

- for vehicle dynamics simulation”, *SAE 970951*.
- Metwally, H.M., Salman, F.K. and EL Lakany, A.M. (1993), “An improved matrix method for the dynamic response for modeling structure under moving vehicles”, *Proceedings of the 11th International Modal Analysis Conference*.
- Mulcahy, N.L. (1983), “Bridge response with tractor-trailer vehicle loading”, *Earthq. Eng. Struct. Dyn.*, **11**, 649-665.
- O’Connor, C. and Pritchard, R.W. (1985), “Impact studies on small composite girder bridges”, *J. Struct. Eng., ASCE*, **111**, 641-653.
- Odman, S.T.A. (1948), “Differential equation for calculation of vibrations produced in load-bearing structures by moving loads”, *International Association for Bridge and Structural Engineering, 3rd congress*, Liege.
- Olsson, M. (1985), “Finite element, modal co-ordinate analyse of structures subjected to moving loads”, *J. Sound Vib.*, **99**, 1-12.
- Schallenkamp, A. (1937), “Schwingungen von tragern bei bewegten lasten”, *Ingenieur-Archiv*, **8**, 182-198.
- Smith, J.W. (1973), “Finite strip analysis of the dynamic response of beam and slab highway bridges”, *Earthq. Eng. Struct. Dyn.*, **1**, 357-370.
- Stauding, A. (1934), “Die Schwingung von Tragern bei bewegten Lasten”, *Ing. Archiv.*, **5**, p.275; *Ing. Archiv.*, **6**, p.265.
- Stokes, G.G. (1896), “Discussions of a differential equation relating to a braking of railway bridges”, *Transactions of the Cambridge Philosophical Society*, **8**, Part 5, p.707.
- Swannell, P. and Miller, C.W. (1987) “Theoretical and experimental studies of a bridge-vehicle system”, *Proceedings of the Institution of Civil Engineers*, **83**, Part 2, 613-635.
- Taheri, M.R. and Ting, E.C. (1989), “Dynamic response of plate to moving loads : structural impedance method”, *Computers and Structures*, **33**, 1379-1393.
- Taheri, M.R. and Ting, E.C. (1990), “Dynamic response of plates to moving loads: finite element method”, *Computers and Structures*, **34**, 509-521.
- Tan, G.H., Brameld, G.H. and Thambiratnam, D.P. (1998), “Development of an analytical model for treating bridge-vehicle interaction”, *Engineering Structures*, **20**(1-2), 54-61.
- Timoshenko, S. (1911), “Erzwungene schwingungen prismatische stabe”, *Math Physik*, **59**, p.163.
- Veletsos, A.S. and Huang, T. (1970), “Analysis of dynamic response of highway bridges”, *J. Eng. Mech. Div., ASCE*, **96**, 593-620.
- Wen, R.K. (1960), “Dynamic response of beams traversed by two-axle loads”, *J. Eng. Mech. Div., ASCE*, **86**, 91-111.
- Willis, R. (1849), *Appendix Report of the Commissioners Appointed to Inquire into the Application of Iron to Railway Structures*, Stationery Office, London. The effect produced by causing weights to travel over elastic bars.
- Wu, J.S., Lee, M.L. and Lai, T.S. (1987), “The dynamic analysis of flat plate under a moving load by the finite element method”, *Int. J. Num. Meth. Eng.*, **24**, 743-762.
- Yang, C.Y. (1986), *Random Vibration of Structures*, John Wiley and Sons, Inc.
- Yang, Y.B. and Yau, J.D. (1997), “Vehicle-bridge interaction element for dynamic analysis”, *J. Struct. Eng., ASCE*, **123**, 1512-1518.
- Zimmermann, H. (1896), “Die Schwingungen eines Tragers mit bewegter Last”, *Centr. Bauverwaltung*, **16**, p. 249.